Trapping parameters estimation of fresh and thermally-aged low-density polyethylene by using an improved trapping/detrapping model

Ning Liu, Ziyun Li, George Chen,
University of Southampton,
Southampton, SO17 1BJ, UK

Mingli Fu, Ruihai Li, Shuai, Hou.
China Southern Power Grid,
Guangzhou, 510000, China.

***Abstract*- In the present paper, trapping parameters of normal and thermally aged low-density polyethylene (LDPE) samples were estimated using the improved charge dynamic model. The results show that, after long-term thermal ageing process, the injection barrier of both electrons and holes is lowered, the overall trap depth is shallower and electron trap density becomes much greater. The latter may indicate that electrons are more sensitive to ageing than those of holes.**

I. INTRODUCTION

During the high voltage application, power loss may lead to a high operation temperature. Consequently, the insulation materials may be subjected to both electric and thermal stresses. For an example, in HV polymeric cables, the insulation layer adjacent to the conductor could work at a temperature up to 90°C. Such thermal stress will accelerate the deterioration of the insulation materials, i.e. ageing and degradation. Especially, in the presence of oxygen, high thermal stress will initiate much more free radicals in the material, thus give rise to oxidation products and eventually cause the acceleration of chemical ageing [1]. As a result of material ageing, charge can be more easily injected into the insulation material and larger local field distortion occurs. In the present paper, space charge was used as a diagnostic tool to evaluate the effect of thermal ageing on polymeric materials. An improved trapping/detrapping model based the previous modelling works [2,3] was utilized to estimate the trapping parameters of normal and thermally-aged LDPE samples.

With space charge dynamics of during depolarization, some previous charge trapping/detrapping models [2,3] have estimated trapping parameters for polyethylene materials. In the present paper, by employing an improved charge trapping/detrapping model, we aim to evaluate the effect of thermal ageing on low-density polyethylene. What different from the previous modelling works [2,3], the new charge trapping/detrapping model makes great strides by considering charge injection process (assumed conforming to Schottky injection), Poole-Frenkel lowering of trap depth and mobile charges moving between trap sites. Moreover, the experimental data of both poling and depoling tests could be used to fit with the developed model. Therefore, trapping parameters could be found with the group of parameters of smallest R-square values.

II. BRIEF ON THE MODEL

The model was initially proposed in our previous paper [4]. It will be briefly described so the extracted trapping parameters can be understood. In the improved model, the observed charges are no longer treated as trapped charges only but include a non-negligible amount of mobile charges as well. Typically, space charge profile with homocharge injection could be divided as positive and negative charge region with thicknesses respectively equalling to d_h and d_e. Therefore, the mean number density of net charges in either region can be calculated as:

$$n_{h,e} = \frac{Q_{h,e}}{d_{h,e}A} \tag{1}$$

where $Q_{h,e}$ is the total charge amount in either charge region and A is the electrode area. The density of net charge $n_{h,e}$ in either region equals to the sum of trapped charge and mobile charge density, i.e.:

$$n_{h,e} = n_{t_{h,e}} + n_{m_{h,e}} \tag{2}$$

where n_t and n_m represent the trapped and mobile charge density respectively in either positive (n_{t_h} and n_{m_h}) or negative charge zone (n_{t_e} and n_{m_e}).

A. Based on single-energy level traps

To assist in establishing the improved model in which new features are introduced, we start with single energy level of traps in the material. The concepts are then extended to the two energy levels of trapping/detrapping processes.

1) Volts-on condition

Here, an assumption has been made that the energy depth of all the traps is on the same level. For instance, in positive charge region, the changing rate for the injected net charge density n_h under the external applied field E can be proposed as:

$$\frac{dn_h}{dt} = \frac{J_h}{qd_h} - Pn_{m_h} - \Delta n'_{m_e} \tag{3}$$

The first term on the right side of Eq. (3) represents the increasing rate of number volumic density of holes coming from the anode by injection. And J_h is the injection current density from the anode. With high voltage applied, charge injection behavior at the metal-insulator interface was verified conforming to Schottky injection mechanism [5]. If the electric field at the interface is E_{i+}(at the anode, or E_{i-} at the cathode), the injection current density J_h at the interface

between the anode and dielectric can be found as [1]:

$$J_h = A_0 T^2 \exp\left(-\frac{qw_h}{kT}\right)\exp\left(\beta_{sc} E_{i+}^{0.5}\right) \quad (4)$$

where A_0 is the constant term, k is Boltzmann constant, T is temperature, ε_0 is the vacuum permittivity, ε_r is the relative permittivity for dielectric, and w_h stands for the original injection barrier height for holes (or w_e for electrons). Normally, *S*chottky constant is written as $\beta_{sc} = \frac{q}{kT}\sqrt{\frac{qE_{i+}}{4\pi\varepsilon_0\varepsilon_r}}$.

When bipolar charges continuously inject into bulk, E_{i+} (or E_{i-}) will be modified. The calculation of E_{i+}(or E_{i-}) will not be shown in the present paper due to the limit of pages, and details can be found in our paper [4].

The second negative term on right side of Eq. (3) describes the decreasing rate of net charge in positive charge layer. Such reduction in the charge layer during voltage-stressing period should be the consequence of the outflow of holes from the local charge region to the opposite electrode. Here, it is postulated that there is a fix portion P (s^{-1}) of mobile charges will outflow from the local charge region.

The third term $\Delta n'_{m_e}$ in Eq. (3) represents increasing rate of the mobile electrons existing in the positive charge region, which are injected from the cathode. To calculate these mobile charges in either space charge region, two situations have to be considered. At every moment, mobile holes of $P_h n_{m_h}$ shall flow from the positive charge region to the other side of bulk meanwhile mobile electrons will flow from the negative region towards the positive charge region with amount of $P_e n_{m_e}$. Detailed calculations of $\Delta n'_{m_{e,h}}$ can be referred to [4].

For the changing rate of positive trapped charge density n_{t_h}, it should consist of three parts, i.e.:

$$\frac{dn_{t_h}}{dt} = -R_{esc} + R_{cap} - R_{rec} \quad (5)$$

Specifically, for the positive charge layer, R_{esc}, R_{cap} and R_{rec} could be expressed as:

$$R_{esc} = n_{t_h} \nu_0 \exp\left(-\frac{E'_{t_h}}{kT}\right) \quad (6)$$

$$R_{cap} = n_{m_h}\left(N_{t_h} - n_{t_h}\right) S_h v_{d_h} \quad (7)$$

$$R_{rec} = B\left(n'_{m_e}\right) n_t \quad (8)$$

In Eq. (6), R_{esc} represents charge escaping rate from traps, ν_0 is the escape attempt frequency, approximating as 2×10^{13} s^{-1} at room temperature [1]. E'_{t_h} is the modified trap depth based on original trap depth E_{t_h} with consideration of Poole-Frenkel lowering ΔV_{pf_h}:

$$E'_{t_h} = E_{t_h} - \Delta V_{pf_h} \quad (9)$$

And the energy barrier lowering ΔV_{pf_h} could be written in the form [1]:

$$\Delta V_{pf_h} = \beta_{pf} E^{0.5} \quad (10)$$

where the Poole-Frenkel constant $\beta_{pf} = 2\beta_{sc}$.

However, in this paper, a modified Poole-Frenkel model [6] has been used, as it is verified to be more suitable for polyethylene material [7]. With such improved Poole-Frenkel model, the averaged barrier lowering considering 3-D effect:

$$\Delta V_{pf_h} = \frac{\int_0^{\frac{\pi}{2}} \beta_{pf}(E\cos\theta)^{0.5}}{\frac{\pi}{2}} = 0.3814\beta_{pf}E^{0.5} \quad (11)$$

Meanwhile, considering increased barrier in the reverse direction of field, the equivalent barrier height lowering $\Delta V'_{pf_h}$ could be found as:

$$\Delta V'_{pf_h} = kT \ln\left[2\cosh\left(\frac{\Delta V_{pf_h}}{kT}\right)\right] \quad (12)$$

The full derivation of Eqs. (11) and (12) will not be shown in the present paper, which could be found in [4] as well.

In Eq. (7), the rate of charge capture R_{cap} by traps will be proportional to the density of mobile holes n_{m_h}, unoccupied trap sites' density $N_{t_h} - n_{t_h}$,where N_{t_h} represents the a total traps density for holes, and v_{d_h} is the drift velocity of charge carriers.

Moreover, we correlate trapping cross section area S_h with trap depth and local electric field [8, 9].

$$S_h = S_0 \left(\frac{E_{t0}}{E'_{t_h}}\right)^2 \left(\frac{E}{E_0}\right)^{-1.5} \quad (13)$$

Details of derivation for equation (13) can be found in [4].

With an averaged drift velocity v_d, the momentum p of the particle moving between two trap sites can be found as:

$$p = m_{h,e} v_d = qE_{\pm} t_d \quad (14)$$

where $m_{h,e}$ is the mass of an electrons or a hole in the material, $E_{\pm}$ is the local electric field under effect of space charge accumulation in the positive charge or negative charge regions, t_d is time of the excited particle moving from one trap to the next. Hence, with a trap separation distance of a, the averaged drift velocity of v_d can be expressed as:

$$v_d = \sqrt{\frac{qE_{\pm}a}{m^*_{h,e}}} \quad (15)$$

Eq. (8) gives the recombination rate of trapped positive charges with accumulated mobile electrons in the positive charge layer, $n'_{m_e} = \int_0^t \Delta n'_{m_e} dt$. This will reduce the trapped charge density in such charge layer.

Similarly, the equations for negative trapped charges can be developed.

2) Volts-off condition

After the removal of external voltage, the Schottky injection at the metal-insulator interface could be neglected because electric field at electrodes E_i included within an exponential term is much lowered. Moreover, in the depolarization stage, charge carriers should move under the field produced by local space charges. For the mobile carriers, the direction of movement should be dependent on the direction of local space charge field, new expression of $\Delta n'_{m_e}$ has to be derived for volts-off condition, see details in our previous paper [4].

Hence, after the removal of external voltage, the changing rate of net charge in positive region becomes:

$$\frac{dn_h}{dt} = -P_h n_{m_h} - \Delta n'_{m_e} \quad (16)$$

For the dynamic equation of trapped charge during depolarization stage, Eqs. (5) – (8) are suitable as well. Moreover, values of field-dependent parameters need to be modified. These include Poole-Frenkel lowering ΔV_{pf_h}, and trapping cross-sectional area S_h . Full expressions and

derivations of the averaged electric fields at both volts-on and volts-off conditions in either charge region can be found in [4].

B. Based on dual-energy level traps

To assign the trapping parameters with more practical meaning relating with physical and chemical defects in the sample, we extend the model from single level to dual energy levels.

By extending the trap depth E_t of model to two energy levels, Eq. (3) becomes:

$$\frac{dn_h}{dt} = \frac{J_h}{qd_h} - Pn_{m_h} = \frac{J_h}{qd_h} - P\left(n - n_{t_{h1}} - n_{t_{h2}}\right) - \Delta n'_{m_e} \quad (17)$$

where $n_{t_{h1}}$ and $n_{t_{h2}}$ represent the positive charges captured at shallow and deep energy levels.

Based on Eqs. (5) – (8), the changing rate of shallow trapped charges in the positive charge layer could be expressed as:

$$\frac{dn_{t_{h1}}}{dt} = -n_{t_{h1}}\nu_0 \exp\left(-\frac{E'_{t_{h1}}}{kT}\right) + n_{m_h}\left(N_{t_{h1}} - n_{t_{h1}}\right)S_{h1}v_{d_h} - Bn'_{m_e}n_{t_{h1}} \quad (18)$$

Likewise, for changing rate of deep trapped positive charges:

$$\frac{dn_{t_{h2}}}{dt} = -n_{t_{h2}}\nu_0 \exp\left(-\frac{E'_{t_{h2}}}{kT}\right) + n_{m_h}\left(N_{t_{h2}} - n_{t_{h2}}\right)S_{h2}v_{d_h} - Bn'_{m_e}n_{t_{h2}} \quad (19)$$

For hole traps at shallow and deep levels respectively, $E'_{t_{h1}}$, $E'_{t_{h2}}$ are the modified trap depth, $\Delta V_{pf_{h1}}$, $\Delta V_{pf_{h2}}$ are the barrier height lowering due to Poole-Frenkel effect, S_{h1},S_{h2} are the capturing cross section area, and v_{d_h} stands for the drift velocity of holes.

III. SAMPLE PREPARATION AND EXPERIMENTAL

Normal additive-free LDPE films were used for space charge measurements and the thickness of samples are 175±10μm. Also, some of the normal LDPE films were aged in fan oven under 90°C for 10 days. The pulsed electroacoustic (PEA) technique was used for observing dynamics of charge profiles and measurements were made for 60 minutes after the removal of the applied voltage.

For LDPE films with slight different thickness, the applied voltage was adjusted so the applied field was fixed at 4×10^7V/m for all the samples. For both normal and thermally aged LDPE samples, two or three consecutive measurements were made and charge amounts from each layer were averaged from those measured data.

IV. SPACE CHARGE RESULT AND CALCULATION OF CHARGE AMOUNT

In Figs. 1(a) - (f), space charge dynamics of both volts-on and volts-off periods using both types of LDPEs are shown. Figs. 1(a) and 1(d) give the space charge dynamics during the volts-on period. In order to obtain the injected space charge in the bulk, subtraction method was employed to eliminate the capacitive charges on two electrodes [10], as in Figs. 1(b) and 1(e). Bipolar charges injection can be observed. After the removal of external voltage, the charge decay result is shown in Figs. 1(c) and 1(f).

Charge amount in the positive charge layer could be found by the following equation:

$$Q_h = \int_{D-d_h}^{D} |n_h(x,t)q| A dx \quad (20)$$

And in the negative layer, it becomes:

$$Q_e = \int_{0}^{d_e} |n_e(x,t)(-q)| A dx \quad (21)$$

With several measured data of both normal and thermally aged LDPE, charge amount in each charge layer can be averaged.

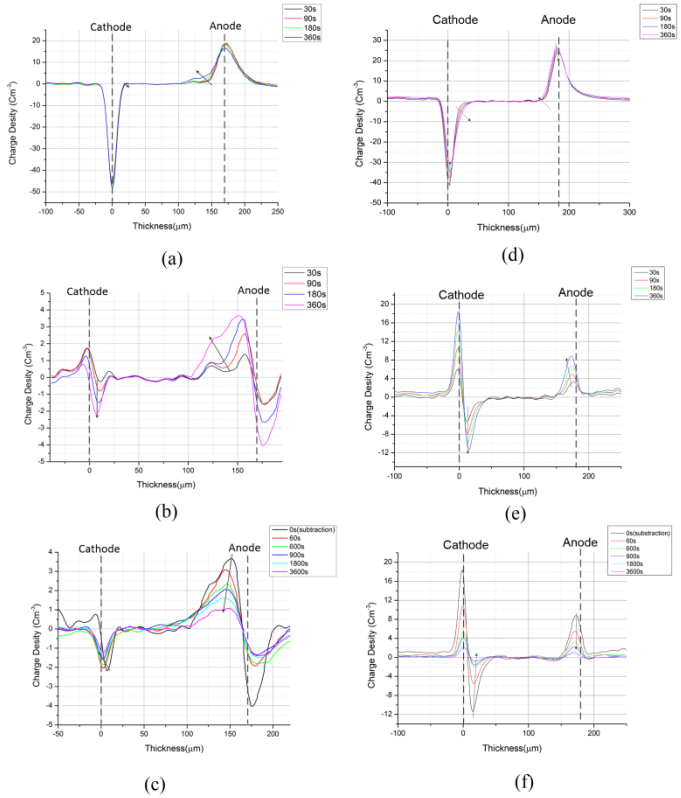

Figure 1: Space charge results of the LDPE samples respectively for normal LDPE (a, b, c), and thermally-aged LDPE (d, e, f): charge dynamics during voltage-stressing period of 6 minutes, (b, e): charge dynamics during voltage-stressing period after subtraction algorithm, (c, f): charge decay dynamic during depolarization stage.

V. SIMULATION RESULTS

A. Model constants

In the present model, some parameters can be treated as constants in accordance with the measured data or the previous literatures, values of which are shown in Table 1.

Table 1: Values of model constants

Model Constant	Value	Model Constant	Values
q(C)	1.60×10^{19}	k(JK^{-1})	1.38×10^{-23}
T(K)	300	$m^*_{h,e}$ (kg)	9.11×10^{-31}
A_0(Am^{-2}K^{-2})	1.20×10^{6}	A(m^2)	6.36×10^{-5}
B(m^{3}s^{-1})	6.40×10^{-19}	v_0 (s^{-1})	2.00×10^{13}

ε_0(Fm^{-1})	8.85×10^{-12}	ε_0(Fm^{-1})	2.3

For thicknesses of positive and negative charge region in the modelling, they are averaged from the measured space charge profiles. Specifically, for lengths of positive charge region and negative, they are 55µm, 20µm for normal LDPE and 37µm, 52 µm for thermal-aged LDPE.

B. Model parameter estimation

In the improved model, for both holes and electrons, typical trapping cross sectional area S_0 , mobile charge escaping rate constant P, injection barrier w and trapping parameters, which include trap density N and depth E_t, have been set as unknown, remaining to be estimated in the simulation. These parameters can be estimated through finding the best curve fitting output between experimental data and numerical solutions, i.e. highest R-square value. The R-square is the square of the correlation between the response values and the predicted response values. With a value closer to 1, it indicates that a greater proportion of variance is accounted for by the model. The highest R-square values for both types of LDPEs determined are as 0.9204 (normal LDPE) and 0.9697 (thermally aged). Fig. 2 gives the optimum numerical solution respectively for poling and depoling charge density data of both normal and thermally aged LDPE samples. In Fig. 2, it is noteworthy that when the applied voltage is switched off, mobile charges start to reduce in each charge layer while trapped charges continue increasing to certain amount then fall (for shallow trapped charges) or almost keep flat (for deep trapped charges). This can be attributed to the trapping cross section area enlargement after the removal of external voltage, i.e. under much weaker field. Thereafter, a number of mobile charges get retrapped into empty sites. However, as the rapid decrease of mobile charges to nearly zero, little charges can be caught into trap sites and detrapping process become predominating in the bulk.

Thus, unknown parameters can be estimated, as shown in Table 2. Additionally, a typical trapping cross-sectional area S_0 is found to be 1.00×10^{-30}m^2 for both electrons and holes.

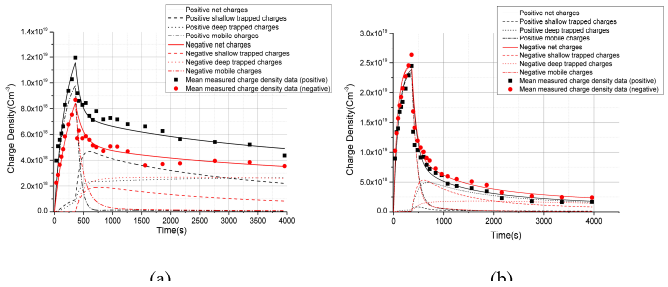

Figure 2: Simulated curves fitting with experimental data of normal LDPE (a) and thermal-aged LDPE (b), based on dual-level model

Comparing model parameters of electrons and holes in Table 2, the changes after thermal ageing can be summarized as:

1. In normal LDPE, the injection barrier of holes is lower than electrons. However, after thermal ageing, injection barrier of electrons become lower than holes'.
2. After thermal ageing, the overall trap depth becomes shallower.
3. Holes' trap density experiences only a little increase after ageing whereas electrons' trap density has a multiplication of more than 30 times.

Table 2: Estimated parameters of both normal and aged LDPE respectively for holes and electrons, using dual-level modelling.

Parameters		Normal LDPE	
		Electrons	Holes
P(s^{-1})		$\mathbf{0.003}$	$\mathbf{0.004}$
w (eV)		$\mathbf{1.224}$	$\mathbf{1.185}$
$\mathbf{E_t}$(eV)	S	$\mathbf{1.004}$	$\mathbf{1.029}$
	D	$\mathbf{1.048}$	$\mathbf{1.073}$
N(m^{-3})	S	$\mathbf{3.82 \times 10^{18}}$	$\mathbf{1.38 \times 10^{21}}$
	D	$\mathbf{4.72 \times 10^{18}}$	$\mathbf{5.43 \times 10^{20}}$
Parameters		Thermal-aged LDPE	
		Electrons	Holes
P(s^{-1})		$\mathbf{0.006}$	$\mathbf{0.007}$
w (eV)		$\mathbf{1.147}$	$\mathbf{1.163}$
$\mathbf{E_t}$(eV)	S	$\mathbf{0.976}$	$\mathbf{0.900}$
	D	$\mathbf{1.024}$	$\mathbf{0.988}$
N(m^{-3})	S	$\mathbf{2.13 \times 10^{20}}$	$\mathbf{1.41 \times 10^{21}}$
	D	$\mathbf{4.37 \times 10^{19}}$	$\mathbf{6.13 \times 10^{20}}$

VI. CONCLUSION

Employing the improved dual-level dynamic model, the behaviour of mobile and trapped charges during volts-on and volts-off period was simulated. Also, estimated injection barrier and trapping parameters were found to be changed by ageing process. However, trap density of electrons can be used as diagnostic tool to monitor ageing with a better sensitivity.

REFERENCES

[1] L. Dissado and J. Fothergill, *Electrical degradation and breakdown in polymers*, 9th ed., edited by P. N. Morgan, D.V. and K. Overshott , Peters Peregrinus Ltd., London, United Kingdom, 1992.

[2] G. Chen and Z. Xu, "Charge trapping and detrapping in polymeric materials," Journal of Applied Physics 106, 123707, 2009.

[3] N. Liu and G. Chen, "Changes in charge trapping/detrapping in polymeric materials and its relation with aging," in Electrical Insulation and Dielectric Phenomena, Annual Report Conference on , Shenzhen,2012.

[4] N. Liu, M. He, H. Alghamdi, G. Chen, M. Fu, R. Li, and S. Hou, "An improved model to estimate trapping parameters in polymeric materials and its application on normal and aged low-density polyethylenes", Journal of Applied Physics, 118, 064102, 2015.

[5] J. Brunson, *Hopping conductivity and charge transport in low density polyethylene*, Ph.D. thesis, Utah State University , 2010.

[6] M. Ieda, G. Sawa, and S. Kato, "A Consideration of Poole-Frenkel Effect on Electric Conduction in Insulators," Journal of Applied Physics 42, 3737–3740, 1971.

[7] G. Raju, *Dielectrics in electric fields*, Marcel Dekker, Inc., New York, United States, 2003.

[8] D. Buchanan, M. Fischetti, and D. DiMaria, "Coulombic and neutral trapping centers in silicon dioxide," Phys. Rev. B 43, 1991.

[9] G. Blaise and W. Sarjeant, "Space charge in dielectrics. energy storage and transfer dynamics from atomistic to macroscopic scale," IEEE Transactions on Dielectrics and Electrical Insulation 5, 779–808, 1998.

[10] N. Liu, C. Zhou, G. Chen, and L. Zhong, "Determination of threshold electric field for charge injection in polymeric materials," Applied Physics Letters 106, 2015.